ELSEVIER

Thermochimica Acta 319 (1998) 105–111

thermochimica
acta

Effect of reactant structure on the solid state reaction between KHF_2 and oxides of iron and vanadium

S.V. Adhyapak-Thosar[1,*], U.R.K. Rao

Applied Chemistry Division, Bhabha Atomic Research Centre, Mumbai 400 085, India

Received 1 July 1997; accepted 1 June 1998

Abstract

Fluoro and oxyfluoro complexes of iron and vanadium were prepared using KHF_2 and their thermal behavior was studied using TG/DTA techniques. All the three oxides of iron reacted with the cubic phase of KHF_2, giving identical products, namely $(NH_4)_3FeF_6\cdot 1.5H_2O$ irrespective of oxidation state of iron. KHF_2 in its tetragonal, as well as cubic phases reacts with vanadium oxide depending on the molar ratio of the reactants. A possible pathway for the thermal degradation is given for the above complexes and the residues obtained were identified. © 1998 Elsevier Science B.V.

1. Introduction

During the last decade, several [1–5] solid state reactions brought about by grinding together the reactants at room temperature have been reported. One of the reactants in these reactions is invariably a hydrogen fluoride of general formula, MHF_2, where $M{=}NH_4^+$, Li^+, Na^+ and K^+, while the other reactant is a vanadate of the general formula MVO_3, where $M{=}NH_4^+$, Li^+, Na^+ and K^+ or a binary oxide, such as V_2O_5, antimony oxide, iron oxide, rare-earth sesquioxide, etc. In all these reactions, by the process of constant grinding of the mixture, a fresh interface (which we refer to as a dynamic interface) between the two reactants is continuously provided to facilitate progress of the reaction. More recently, solid state reaction between the same pairs of solids as above, but brought about by keeping them in contact with each other at a fixed interface (which we shall refer to as static interface), was reported [6–9]. Once the product is formed, further reaction can take place at the static interface only by the transport of one or both reactants across the product layer. In all the above pairs of reactants, it was noticed that only MHF_2 moved across the ever growing product layer at the interface. Among the above pairs of reactants, although in some cases the reaction readily takes place at a dynamic interface, it does not progress beyond the formation of a thin layer of the product layer at the static interface. A case in point is the reaction between KHF_2 and KVO_3. This was attributed to structural features, such as packing efficiency of the product, $K_3VO_2F_4\cdot H_2O$, which does not allow the KHF_2 to transport across it into KVO_3 layer for further reaction.

In this communication, yet another basic aspect of reactivity between two solids, namely the structure of reactants, is probed. Unlike NH_4HF_2, KHF_2 has a tetragonal-to-cubic crystallographic phase transition at 198°C. In its tetragonal phase, KHF_2 reacts at room

---

*Corresponding author. Fax: 91-22-556-0750; e-mail: sichem@magnum.barc.ernet.ins

[1] Present address: The Institute of Science, Dept. of Chemistry, Inorganic Chemistry Section, Madam Cama Road, Mumbai 400 032, India.

PII S0040-6031(98)00395-5

temperature with $(NH_4/Na)VO_3$ to form crystalline product $K_2(NH_4/Na)VO_2F_4{\cdot}H_2O$ at a dynamic interface [7]. However, the same KHF_2 either in its tetragonal or cubic phase does not react with $(Nb/Ta)_2O_5$, but reacts only at its melting point [10].

The reaction between NH_4HF_2 and oxides of iron, namely α-Fe_2O_3, Fe_3O_4 and γ-Fe_2O_3 at dynamic interface has already been reported [5]. In this communication, the reactivity of KHF_2 in its two modifications towards oxides of iron and vanadium is examined.

2. Experimental

The oxides of iron used were: α-Fe_2O_3 of Qualigens Fine Chemicals, LR grade, preheated to 700°C in air, and Fe_3O_4 from Aldrich. γ-Fe_2O_3 was prepared by heating Fe_3O_4 at 120°C in air for 7 days. KHF_2 and KF were of AR grade dried at 80°C prior to use. V_2O_5 used was of BDH LR grade. VO_2 was prepared by heating vanadyl oxalate in an inert atmosphere at 385°C for 1 h [11]. Powder XRD patterns were run on a Philips APD machine model PW 1729 employing Ni-filtered CuK_α radiation. The simultaneous TG–DTA used was ULVAC SINKU RIKO TGD model 7000 RHP. The sample size was ca. 35 mg with the heating rates 6–10°C/min and an atmosphere of static air.

The oxides were mixed with KHF_2 or KHF_2/KF mixture, as the case may be, in the stoichiometry given in Table 1. The mixture, $\approx$1 g, was ground in a polythene bag with a pestle for about half-an-hour at room temperature and stored in a desiccator over P_2O_5. Part of the mixture was taken out periodically and the progress of the reaction monitored by the powder XRD technique. In case there was no reaction at ambient temperature for a day, fresh mixtures were heated isothermally in a DTA setup at a temperature 50°C higher than the ambient. The ^{57}Fe Mössbauer spectra of the products obtained from the reaction with iron oxides, were recorded at room temperature as described earlier [5].

3. Results and discussion

3.1. Reaction

In case of the three mixtures, A, B and C of oxides of iron, it was observed that, even after 72 h of mixing, the reaction had not been initiated, as the XRD pattern showed lines of only the reactants. This behaviour is at variance with the one [5] observed by us in the case of reaction between NH_4HF_2 and the two oxides of iron, namely Fe_3O_4 and γ-Fe_2O_3, wherein the reaction proceeded to completion within a few hours at the ambient temperature itself.

The mixtures, A, B and C were heated isothermally in the DTA furnace at different temperatures up to the melting point of KHF_2 to investigate whether the reaction took place at all.

Fresh mixtures were heated at 100°, 125° and 150°C for 3 h and cooled to room temperature, when it was observed that no new lines appeared in the XRD pattern in all three cases. A fresh mixture was heated at 200°C for 4 h and cooled to room temperature with the XRD pattern showing complete formation of the known complex [12], $K_3FeF_6{\cdot}1.5H_2O$. This was supported by the absence of an endotherm at 198° and

Table 1

Mixture	Oxide	Mixture mole ratio			Product formed
		Oxide	KHF_2	KF	
A	α-Fe_2O_3	1	6	—	$K_3FeF_6{\cdot}1.5H_2O$
B	Fe_3O_4	1	9	—	$K_3FeF_6{\cdot}1.5H_2O$
C	γ-Fe_2O_3	1	6	—	$K_3FeF_6{\cdot}1.5H_2O$
D	V_2O_5	1	2	—	$KVO_2F_2{\cdot}0.5H_2O$
E	V_2O_5	1	2	2	$K_2VO_2F_3{\cdot}0.5H_2O$
F	V_2O_5	1	2	4	$K_3VO_2F_4$
G	V_2O_5	1	6	—	K_3VOF_6
H	VO_2	1	2	1	K_3VOF_5

225°C in the DTA, due to a phase transition and melting of KHF_2, when this product was reheated to 250°C. This compound was earlier prepared by Peacock [12] by adding a solution of $FeCl_3$ in HF to a solution of KF with an excess of HF at room temperature.

In the case of mixture B, on heating at 150°C for 3 h and cooling to room temperature, the XRD pattern showed partial formation of the same complex, K_3FeF_6, along with some unreacted starting materials. The reaction goes to completion at 200°C in cubic phase of KHF_2 when held for 2 h, giving K_3FeF_6. In this reaction with KHF_2, just as in the case of NH_4HF_2 [5], the Fe^{2+} part of Fe_3O_4 was oxidised to Fe^{3+} during the reaction. However, in the case of reaction with KHF_2 there is an additional factor of heating in air up to 200°C. It was ascertained in an independent experiment that Fe_3O_4, when heated alone for 2 h in air up to 200°C, retains its Fe^{2+} part. Thus, the Fe^{2+} part of Fe_3O_4 was oxidised to Fe^{3+} only during the reaction with KHF_2 at 200°C.

Similarly, KHF_2 reacts with α-Fe_2O_3 partially at $T<200°C$ and the reaction is completed within 2 h at 200°C, i.e. above the phase-transition temperature of KHF_2. The product obtained was the same as in the above two cases.

The ^{57}Fe Mössbauer Spectra of all the products of the three mixtures are identical. It is a singlet having an isomeric shift of 0.39±0.01 mm/s in agreement with the reported [13] value of 0.39 mm/s for FeF_6^{3-} ion.

In the case of mixtures D and E of V_2O_5, it was observed that the reaction goes to completion at room temperature itself. The hitherto unknown XRD pattern observed in the case of mixture D is shown in Fig. 1 and was assumed to be due to $KVO_2F_2\cdot0\cdot5H_2O$ analogous to $NH_4VO_2F_2\cdot0\cdot5H_2O$ formed by solid state reaction between 1 mol of V_2O_5 and 2 mol of NH_4HF_2 [14]. It could be indexed based on an orthorhombic unit cell as given in Table 2. The XRD pattern of the mixture E corresponds to the known complex $K_2VO_2F_3\cdot0\cdot5H_2O$ reported by Pausewang et al. [15].

On the other hand, the mixtures F and G showed incomplete reaction when kept at room temperature even after a day after mixing. This can be ascertained from the lines due to reactants seen from in the XRD pattern. Hence, the mixture was heated at different temperatures up to 180°C but the reaction did not progress. However, at 210°C in the cubic form of KHF_2, the reaction goes to completion. The XRD patterns of the products F and G are identical and are assumed to be due to $K_3VO_2F_4$ and K_3VOF_6, respectively. They are indexed on the basis of a tetragonal unit cell [15]. To differentiate between these two complexes, the fluoride content was estimated in two different ways, one by Fluoride ion selective electrode method and other by titrimetric method [16]. The results are given in Table 3.

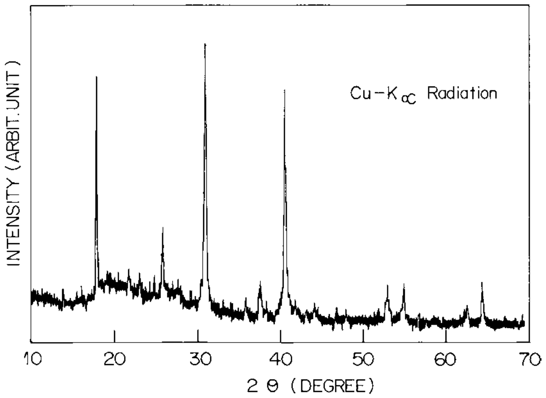

Fig. 1. Powder XRD pattern of $KVO_2F_2\cdot0.5H_2O$.

Table 2
Fit of powder XRD pattern of $KVO_2F_2\cdot0.5H_2O$

d obs/Å	d cal/Å	h	k	l	I/I_o/%
5.004	5.001	1	1	0	85
3.453	3.451	0	2	2	10
3.243	3.241	2	0	0	25
2.925	2.925	1	1	4	30
2.885	2.886	0	0	5	100
2.500	2.449	1	1	5	10
2.393	2.395	1	3	1	20
2.361	2.362	2	2	2	10
2.219	2.218	2	2	3	80
2.038	2.037	2	3	0	15
1.727	1.725	0	4	4	15
1.670	1.669	2	4	1	10
1.486	1.485	0	3	8	10
1.441	1.441	0	5	4	20

Note: System – Orthorhombic.
a_o =6.482±0.003 (Å).
b_o =7.861± 0.002 (Å).
c_o =14.430±0.005 (Å).

Mixture H, when heated at 210°C in an inert atmosphere to prevent oxidation of V(IV) in air, gave the

Table 3
Results of fluorine estimation

Compound	F-content/wt. %)			
	Titrimetry method		F-ion selective electrode method	
	Obs	Cal	Obs	Cal
K_3VOF_6	(i) 33.20 (ii) 33.63	35.05	(i) 34.20 (ii) 33.85	35.05
$K_3VO_2F_4$	(i) 25.50 (ii) 26.15	26.65	(i) 26.10 (ii) 25.92	26.65

complex K_3VOF_5. This complex was prepared by Baker and Haendler from an aqueous HF solution route [17].

3.2. TG/DTA

3.2.1. $K_3FeF_6 \cdot 1.5H_2O$

The simultaneous TG/DTA run of K_3FeF_6 is shown in Fig. 2. From the TG, the weight loss of 8.5% observed up to 110°C may be attributed to removal of occluded water. The corresponding DTA shows an endotherm at 110°C. However, no further weight loss in the TG or presence of any other peak in the DTA was observed up to 810°C. The TG showed continuous loss in weight beyond 810°C. The corresponding DTA run showed a sharp endotherm at 810°C followed by a continuous deviation from the base line. The endotherm at 810°C was reversible on thermal cycling and XRD continued to show the presence of the complex along with some α-Fe_2O_3. The amount of the oxide formed increased at the expense of the complex as the number of thermal cyclings through 810°C increased. The residue obtained at 900°C was only the ferric oxide. This shows that the complex melts at 810°C with concomitant onset of decomposition. The overall decomposition is envisaged to proceed as follows:

$$K_3FeF_6 \cdot 1.5H_2O \rightarrow FeO_{1.5} + 3KF + 3HF$$

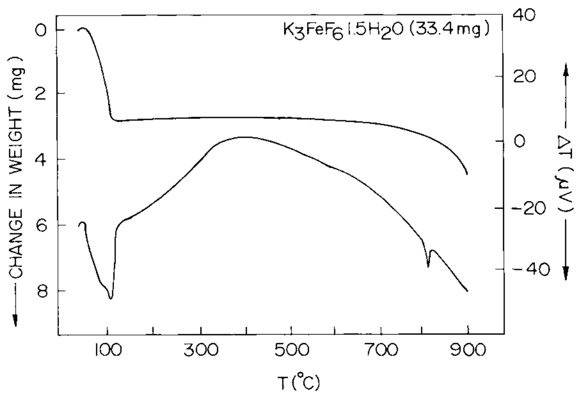

Fig. 2. Simultaneous TG/DTA scan of K_3FeF_6.

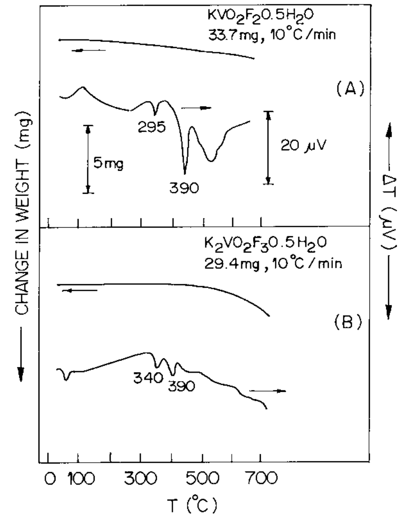

Fig. 3. Simultaneous TG/DTA scan of (i) $KVO_2F_2 \cdot 0.5H_2O$; (ii) $K_2VO_2F_3 \cdot 0.5H_2O$.

3.2.2. $KVO_2F_2 \cdot 0.5H_2O$

The TG/DTA scan of $KVO_2F_2 \cdot 0.5H_2O$ is shown in Fig. 3. TG shows continuous weight loss. DTA showed two endotherms at 295 and 390°C. The second endotherm was found to be reversible. The XRD pattern of the sample heated to 300°C showed the lines of the starting compound, $K_2VO_2F_3$ and KVO_3. On further heating at 400°C, the XRD pattern showed presence of lines due to $K_3VO_2F_4$ and KVO_3. When the sample was heated at 600°C, it overflowed out of sample holder (TG/DTA cup) and DTA run beyond 600°C could not be recorded. A fresh sample was heated separately in platinum boat in furnace at 900°C and its XRD pattern showed lines of only KVO_3 with high background. Thus, the first endotherm can be attributed to decomposition of $KVO_2F_2 \cdot 0.5H_2O$

whereas the second endotherm to melting of $K_2VO_2F_3{\cdot}0.5H_2O$, formed during decomposition of $KVO_2F_2{\cdot}0.5H_2O$. The $K_2VO_2F_3{\cdot}0.5H_2O$ decomposes after melting to give KVO_3 and $K_3VO_2F_4$ which on further heating decomposes to give KVO_3 and KF. The thermal degradation can be written as,

$$4KVO_2F_2 \cdot 0.5H_2O \xrightarrow{300^\circ C} 2K_2VO_2F_3 \cdot 0.5H_2O + V_2O_5 + 2HF \qquad (1)$$

$$2K_2VO_2F_3 \cdot 0.5H_2O \xrightarrow{400^\circ C} K_3VO_2F_4 + KVO_3 + 2HF \qquad (2)$$

$$K_3VO_2F_4 + H_2O \xrightarrow{>400^\circ C} KVO_3 + 2KF + 2HF \qquad (3)$$

Overall,

$$4KVO_2F_2 \cdot 0.5H_2O + H_20 \rightarrow 2KVO_3 + V_2O_5 + 2KF + 6HF \qquad (4)$$

A similar scheme of decomposition of $K_2LiVO_2F_4H_2O$ involving $K_3VO_2F_4H_2O$, KVO_3 and LiF as intermediates was also arrived by Patwe et al. [18].

3.2.3. $K_2VO_2F_3{\cdot}0.5H_2O$

The TG scan of $K_2VO_2F_3{\cdot}0.5H_2O$ showed that compound is thermally stable up to 400°C. Its DTA showed (Fig. 3) two endotherms one at 340°C and other at 390°C. The endotherm at 340°C is reversible and appeared at 290°C while cooling. The XRD pattern of the compound heated to 350°C and cooled, showed the lines due to parent compound only. Thus, it can be inferred that the compound undergoes a reversible phase transition at 340°C. A fresh sample heated to 400°C and cooled to room temperature showed the lines due to parent compound, $K_3VO_2F_4$ and KVO_3. Thus, $K_2VO_2F_3{\cdot}0.5H_2O$ first melts at 390°C and then decomposes (vide Eq. (2)). This compound on further heating gets decomposed completely since the residue at 700°C is identified as mixture of KVO_3 and KF. So the thermal degradation can be represented by the above Eqs. (2) and (3). The overall degradation can be given as,

$$2K_2VO_2F_3 \cdot 0.5H_2O \rightarrow 2KVO_3 + 2KF + 2HF \qquad (5)$$

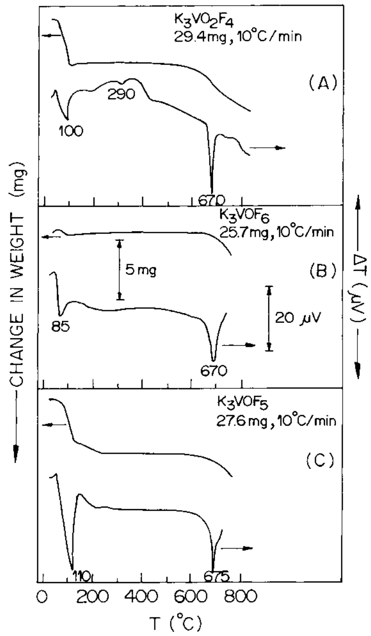

Fig. 4. Simultaneous TG/DTA scan of (i) K_3VOF_6; (ii) $K_3VO_2F_4$; (iii) K_3VOF_5.

3.2.4. $K_3VO_2F_4$

The simultaneous TG/DTA scan of the compound is shown in Fig. 4(A). The initial 6% weight loss observed in TG may be due to loss of occluded moisture which is shown in DTA curve as an endotherm at 90°C. $K_3VO_2F_4$ is thermally stable up to 600°C and then gradually loses weight above this temperature. A small endotherm is observed at 290°C due to a phase transition as shown elsewhere by EPR and DSC [19]. The strong endotherm observed at 670°C, attributed to melting of $K_3VO_2F_4$, was found to be reversible while cooling. The XRD pattern showed the lines due to starting material and KVO_3. The amount of KVO_3 formed increased at the expense of the parent compound as the number of thermal cyclings through 670°C increased. A sample of the parent compound separately heated to 900°C in air and cooled to room temperature gave a mixture of KVO_3 and KF. The thermal degradation of this compound at 900°C may be written as follows:

$$K_3VO_2F_4 + H_2O \xrightarrow{>600^\circ C} KVO_3 + 2KF + 2HF \qquad (6)$$

3.2.5. K_3VOF_6

The simultaneous TG/DTA scan of K_3VOF_6 is shown in Fig. 4(B). TG shows plateau up to 600°C. After this temperature continuous weight loss is observed. DTA shows reversible endotherm at 670°C due to melting of K_3VOF_6. The XRD pattern of the compound heated to 670°C and cooled, showed the lines due to starting compound and KVO_3. The residue obtained at 900°C was KVO_3. The decomposition may be envisaged as follows,

$$K_3VOF_6 + 2H_2O \rightarrow KVO_3 + 2KF + 4HF \tag{7}$$

3.2.6. K_3VOF_5

The simultaneous TG/DTA curve of this product is shown in Fig. 4(C). The initial weight loss observed in TG is due to loss of occluded moisture. The corresponding endo is reflected at 110°C in DTA. The compound is thermally stable up to 650°C. Weight loss is observed continuously after this temperature. An endotherm in DTA at 675°C is due to melting of the compound. The XRD of the residue showed the lines of V_2O_5. Thus, the thermal degradation can be given as,

$$2K_3VOF_5 + 2H_2O + 0.5O_2 \rightarrow V_2O_5 + 6KF + 4HF \tag{8}$$

The peak at 675°C may be due to melting of V_2O_5 (m.p. 690°C).

4. Conclusion

From the above, it was concluded that the three oxides of iron do not react with KHF_2 in its tetragonal form when heated up to 150°C. However, all three oxides readily react with KHF_2 in the cubic form to give the identical product, i.e. K_3FeF_6.

This study clearly brings out the most striking indication of reactivity of solids, namely the role of structure of one of the solids, namely KHF_2. The KHF_2 in its tetragonal form does not react at 190°C, just below the transition temperature, while it readily reacts in its cubic form at 210°C, just above the transition temperature. Here, kT cannot explain the difference in reactivity of KHF_2 at two close temperatures but for their structures. This aspect was earlier indicated in our studies [6] wherein it was mentioned that although all the rare-earth sesquioxides have more or less same unit cell dimension and same structure, the solid state reactivity of KHF_2 towards them is different. KHF_2 reacts with some of these oxides in its tetragonal form while it reacts with some other oxides only in its cubic form and with still other oxides at its melting point only.

In the case of vanadium oxides, KHF_2 in its tetragonal form either by itself or along with KF reacts with V_2O_5 at room temperature itself and depending on the molar ratios of the reactants it gives the complexes $KVO_2F_2{\cdot}0.5H_2O$ and $K_2VO_2F_3{\cdot}0.5H_2O$. V_2O_5 and VO_2 react with KHF_2 above 200°C in the cubic form and depending on the molar ratios of reactants, the products are K_3VOF_6, $K_3VO_2F_4$ and K_3VOF_5. The effect of temperature alone cannot explain the difference in reactivity of KHF_2 since the enhancement in kT is not all that significant on going over from 150° to 200°C. Hedvall effect [20] may be invoked to explain the reactivity of KHF_2 in its different crystallographic modifications.

Acknowledgements

The author thanks Dr Satya Brat for the thermal data and Dr S.K. Kulshrestha for the Mössbauer data and also thanks Dr P.N. Moorthy, Associate Director, Chemistry Group for his interest in the work.

References

[1] U.R.K. Rao, K.S. Venkateswarlu, B.N. Wani, J. Fluorine Chem. 31 (1986) 29.

[2] S.J. Patwe, B.N. Wani, U.R.K. Rao, K.S. Venkateswarlu, Can. J. Chem. 67 (1989) 1815.

[3] B.N. Wani, S.J. Patwe, U.R.K. Rao, K.S. Venkateswarlu, J. Fluorine Chem. 44 (1989) 177.

[4] B.N. Wani, U.R.K. Rao, Syn. and React. in Inorg. and Org-Met Chem. 21 (1991) 179.

[5] S.V. Adhyapak, B.N. Wani, U.R.K. Rao, S.K. Kulshreshtha, Syn. and React. in Inorg. and Org-Met Chem. 22 (1992) 732.

[6] B.N. Wani, U.R.K. Rao, J. Solid State Chem. 112 (1994) 199.

[7] B.N. Wani, S.J. Patwe, U.R.K. Rao, Current Science 62 (1992) 297.

[8] B.N. Wani, U.R.K. Rao, Mat. Chem. and Physics 33 (1993) 165.

[9] J.G. Shah, V.A. Patki, K. Shivkami, B.N. Wani, S.J. Patwe, U.R.K. Rao, Applied Phy. Commun. 12 (1993) 141.

[10] A.I. Agulyanskii, S.S. Pochivalov, V.M. Melnikova, Z. Neorg. Khim. 34 (1989) 2740.

[11] D.N. Satyanaryana, C.C. Patel, J. Inorg. Nucl. Chem. 27 (1965) 297.

[12] R.D. Peacock, J. Chem. Soc., (1957) 4684.

[13] N.L. Costa, J. Danon, R. Moriara Xavier, J. Phys and Chem. Solids 23 (1962) 1783.

[14] U.R.K. Rao, K.S. Venkateswarlu, B.N. Wani, Thermo. Chem. Acta 81 (1984) 23.

[15] G. Pausewang, K. Dehnicke, Z. Anorg. Allg. Chem. 369 (1969) 265.

[16] H.H. Willard, O.B. Winter, Ind. Eng. Chem. Anal., Ed 5 (1933) 7.

[17] A.E. Baker, H.M. Haendler, Inorg. Chem. 1 (1962) 127.

[18] S.J. Patwe, Ph.D Thesis University of Bombay (1993).

[19] S.V. Adhyapak, R.M. Kadam, A.G. Page, U.R. K Rao, Phase transistion 51 (1994) 199.

[20] Hedvall, Reaktionsfahigkeit fester. Stoffe, Leipzig (1938), Cited in W.E.Garner, Chemistry of Solid State, Butterworths Scientific Publications London (1955).